



HAL
open science

Temperature Derating and Photovoltaic Efficiency in Urban Climates: A Case Study of Sydney Metropolitan Region

Alessia Boccalatte, Christophe Ménézo, Martin Thebault, Julien Ramousse,
Marco Fossa

► To cite this version:

Alessia Boccalatte, Christophe Ménézo, Martin Thebault, Julien Ramousse, Marco Fossa. Temperature Derating and Photovoltaic Efficiency in Urban Climates: A Case Study of Sydney Metropolitan Region. 6th International Conference on Countermeasures to Urban Heat Islands 4 - 7 December 2023 Melbourne, Australia, Priyadarsini Rajagopalan, Veronica Soebarto, Hashem Akbari, Dec 2023, Melbourne, France. hal-04845130

HAL Id: hal-04845130

<https://cnrs.hal.science/hal-04845130v1>

Submitted on 18 Dec 2024

HAL is a multi-disciplinary open access archive for the deposit and dissemination of scientific research documents, whether they are published or not. The documents may come from teaching and research institutions in France or abroad, or from public or private research centers.

L'archive ouverte pluridisciplinaire **HAL**, est destinée au dépôt et à la diffusion de documents scientifiques de niveau recherche, publiés ou non, émanant des établissements d'enseignement et de recherche français ou étrangers, des laboratoires publics ou privés.

Temperature Derating and Photovoltaic Efficiency in Urban Climates: A Case Study of Sydney Metropolitan Region

Alessia, Boccalatte¹, Christophe, Ménézo², Martin, Thebault³, Julien, Ramousse⁴, Marco, Fossa⁵

^{1,2,3,4}*LOCIE, Université Savoie Mont Blanc, CNRS, UMR5271, Le Bourget du Lac, France*

^{1,5}*DIME-Department of Mechanical, Energy, Management and Transportation Engineering, University of Genoa, Genoa, Italy*

ABSTRACT

This study examines the performance of photovoltaic (PV) installations in different areas near Sydney (NSW) by analyzing meteorological data from ten weather stations. The Sandia PV array performance model is utilized to analyze the thermal and electrical performance of four distinct PV module installation conditions. Results indicate that extremely hot weather conditions significantly reduce module efficiency, with close roof mount and insulated back configurations exhibiting lower performance than the open-rack configuration. PV cell operating temperatures can reach hourly peaks ranging from 60°C, for the open rack mount, to more than 90°C for the insulated back. Temperature derating, defined as the deviation of PV power output from the standard test cell temperature conditions ($T_c=25^\circ\text{C}$), can reach hourly peaks of about -40% for the insulated back configuration. A strong negative linear correlation ($R\text{-Pearson}=-0.79$) is observed between PV performance ratio and cooling degree hours, with extreme hot weather conditions having a significant impact on both PV performance and demand for cooling. The open rack configuration demonstrates the highest power production, while the insulated back configuration leads to decreased power production up to 9.5% in summer and 8.3% annually in relation to Sydney, NSW.

Keywords: PV Performance, Urban Environment, Temperature Losses.

Introduction

Urbanization has led to the emergence of urban heat islands (UHIs) in cities, resulting in higher temperatures, particularly during heatwaves (Founda & Santamouris, 2017; Nadeem, Tariq, Haq, & Khan, 2022). This has negative implications for energy systems, especially photovoltaic (PV) installations on buildings (Berardi & Graham, 2020). PV systems are adversely affected by high temperatures, which are exacerbated by UHIs (Yupeng Wang, Berardi, & Akbari, 2016). UHIs can reach up to 4°C or more during the day, contributing to increased PV cell temperatures (Hibbard, Hoffman, Huntzinger, & West, 2017). The limited space in urban areas forces PV modules to be installed on rooftops, where urban air temperatures are higher, leading to reduced performance (Yiping Wang et al., 2006). In this regard, of particular concern are insulated back (Building Integrated Photovoltaics BIPV) and close roof mount configurations, which are particularly vulnerable to increased temperatures (Sailor, Anand, & King, 2021).

In Australia, rooftop PV dominates the market, with over 3 million installations by the end of 2021. PV systems power over 33% of standalone households (Koschier & Egan,

¹ Corresponding Author: alessia.boccalatte@univ-smb.fr, 0000-0003-2620-8750

2021). Despite favorable insolation levels in Sydney, extreme summer temperatures create thermal discomfort for PV systems. Standard Test Conditions (STC) rate PV modules at 25°C ambient temperature, significantly lower than typical Australian summer conditions. Moreover, Sydney temperatures are rising (Livada et al., 2019), with projected increases in maximum air temperature (Matthew Adams, 2015). Previous studies demonstrate that Sydney metropolitan region experiences varying UHI intensities, with average maximum intensity exceeding 6°C (Santamouris et al., 2017). Additionally, elevated PV module surface temperatures can contribute to surface urban heat islands (SUHIs), exacerbating the urban heat issue (Barron-gafford et al., 2016).

This study aims to investigate the impact of local climate conditions and mounting configurations on PV thermal response and efficiency, focusing on extreme hot weather and rooftop PV installations in the Sydney metropolitan region. Hourly temperature and wind speed data from ten nearby weather stations recorded by the Australian Bureau of Meteorology between 2016 and 2017 are analyzed using the Sandia PV array performance model (King, Boyson, & Kratochvil, 2004).

Methodology

This study aims to analyse the performance of photovoltaic installations located in different areas near the city of Sydney, NSW, Australia. Meteorological data recorded from the Australian Bureau of Meteorology (BOM) between 2016 and 2017 from ten weather stations (shown in Figure 1) are considered for the analysis.

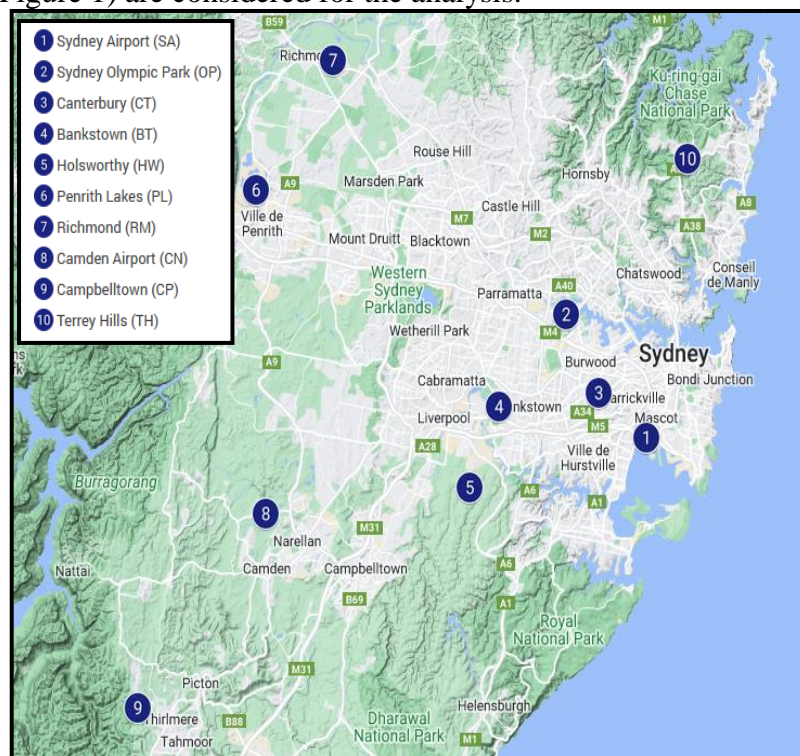


Figure 1. Analysed weather stations near Sydney

To effectively analyze the performance of photovoltaic (PV) modules under various microclimatic conditions, it is essential to consider the electricity demand over the course of a day. One useful indicator of electricity demand for cooling purposes is Cooling Degree Hours (CDH). CDH is calculated as the sum of the positive hourly differences between the outdoor air temperature and a base temperature, which is typically set at 19.5°C based on the

Australian Energy Market Operator (AEMO) guidelines for New South Wales. The formula for calculating CDH is described in Eq. 1

$$CDH = \sum_{i=1}^N (T_{air} - T_{ref}) \quad \text{for } T_{air} > T_{ref} \quad (1)$$

Here, N is the number of hours over a selected time period (day, month, year), T_{air} is the hourly air temperature, and T_{ref} is the reference base temperature.

The Sandia PV array performance model (King et al., 2004) is used to analyze the thermal and electrical performance of four different photovoltaic module mounting possibilities: open rack (OR) with glass/cell/glass (gg) and glass/cell/polymer (gp) module type, close roof mount (CM) with glass/cell/glass (gg), and insulated back (IB) with glass/cell/polymer (gp). The photovoltaic modules considered in the analysis are inclined at an angle of 28 degrees and oriented towards north, being the selected tilt both close to the best angle for yearly energy yield and to the slope of roofs in the Sydney area.

The Sandia model is used to calculate the operating temperature of the photovoltaic modules (T_c) as a function of the considered configuration in each weather station based on Eq. 2

$$T_c = T_m + \left(\frac{G_{POA}}{G_{STC}} \right) \cdot \Delta T \quad (2)$$

Where G_{POA} is the plane of array (POA) irradiance incident on module surface [W/m^2], G_{STC} is the irradiance at Standard Test Conditions (STC), namely $1000 W/m^2$, ΔT is the temperature difference [$^{\circ}C$] between the cell and the back surface at G_{STC} irradiance level, and T_m is the back-surface module temperature [$^{\circ}C$] which can be calculated based on Eq. 3

$$T_m = G_{POA} \cdot \{e^{a+b \cdot WS}\} + T_a \quad (3)$$

Where WS is the wind speed [m/s], T_a is the ambient air temperature [$^{\circ}C$], and a and b are empirically determined coefficients depending on the module type and the mounting configuration. ΔT , a, and b can be derived from Table 1

Table 1. Modelling parameters based on module type and mounting configuration

Module type	Mount	a	b	ΔT ($^{\circ}C$)
Glass/cell/glass	Open rack	-3.47	-0.0594	3
Glass/cell/glass	Close roof mount	-2.98	-0.0471	1
Glass/cell/polymer sheet	Open rack	-3.56	-0.0750	3
Glass/cell/polymer sheet	Insulated back	-2.81	-0.0455	0

The calculation of the DC power output at the maximum power point (P_{mp}) is composed of a set of equations, which are fully detailed in (King et al., 2004) and not reported here for the sake of brevity.

The impact of high temperature conditions on the electrical performance of the considered PV installations is analyzed in terms of efficiency, normalized efficiency, temperature derating, performance ratio, and photovoltaic production.

The PV module efficiency η_{PV} is calculated as in Eq. 4

$$\eta_{PV}(t) = \frac{P_{mp}(t)}{G_{POA}(t)} \quad (4)$$

where P_{mp} is the DC power generated by the PV array system [W/m^2] and G_{POA} is the plane of array (POA) irradiance received by the module [W/m^2].

The normalized efficiency η_N is defined as in Eq. 5

$$\eta_N(t) = \frac{P_{mp}(t) \cdot \frac{1}{P_{STC}}}{G_{POA}(t) \cdot \frac{1}{G_{STC}}} \quad (5)$$

Where P_{STC} is the rated PV power at Standard Test Conditions (STC) of $G_{STC}=1000$ W/m^2 , $T_c=25^\circ C$, and $AM_a=1.5$.

To quantify the impact of high temperatures on PV production the temperature derating (TD) is defined as in Eq. 6

$$TD = \frac{P_{mp}(t) - P_{25}(t)}{P_{mp}(t)} \quad (6)$$

Where P_{25} is the theoretical DC power of the PV array system [W/m^2] at STC cell temperature, namely $T_c=25^\circ C$.

Similarly to the normalized efficiency the performance ratio PR represents the ratio between the Final Yield $Y_{f,\tau}$ and the Reference Yield $Y_{r,\tau}$ over a time interval τ (typically a day) as in Eq. 7

$$PR_\tau = \frac{Y_{f,\tau}}{Y_{r,\tau}} = \frac{\frac{1}{P_{STC}} \cdot \sum_\tau P_{mp}(t) \cdot \Delta t}{\frac{1}{G_{STC}} \sum_\tau G_{POA}(t) \cdot \Delta t} \quad (7)$$

Results and Discussion

Weather conditions at the different weather stations

Table 2 presents summary statistics of air temperature and wind speed values for each weather station. The data is collected from 11 different weather stations identified by their ID, namely Bankstown (BT), Camden Airport (CN), Campbelltown (CP), Canterbury (CT), Holsworthy (HW), Sydney Olympic Park (OP), Penrith Lakes (PL), Richmond (RM), Sydney Airport (SA), and Terrey Hills (TH). Looking at the mean air temperature values, it can be seen that the Sydney Airport (SA) weather station has the highest mean temperature of $19.2^\circ C$, while the Campbelltown (CP) station has the lowest mean temperature of $17.1^\circ C$. The standard deviation of air temperature values also varies significantly among stations, ranging from $5.2^\circ C$ for the Sydney Airport (SA) station to $7.2^\circ C$ for the Richmond (RM) station. The maximum air temperature values range from $39.6^\circ C$ for the Terrey Hills (TH) station to $46.4^\circ C$ for the Penrith Lakes (PL) station, while the minimum values range from $-1.7^\circ C$ for the Camden Airport (CN) station to $5.7^\circ C$ for the Sydney Airport (SA) station. Regarding wind speed, the Sydney Airport (SA) station again shows the highest mean value of 5.7 m/s, while the Campbelltown (CP) station has the lowest mean value of 2.1 m/s. The maximum wind speed values range from 8.2 m/s for the CP station to 16.0 m/s for the Sydney Airport (SA) station. The influence of the sea breeze in the Sydney metropolitan region is important in cooling the coastal areas of the city. However, this cooling effect is limited in its reach, particularly in the western regions of the city located at the base of the mountains. As a result, these areas, such as Penrith Lakes (PL) can experience extremely high temperatures, which can exacerbate the negative impacts of UHIs on urban environments and PV systems.

Table 2. Summary statistics of air temperature and wind speed values for each weather station

Weather station ID										
	BT	CN	CP	CT	HW	OP	PL	RM	SA	TH
Air Temperature [°C]										
mean	18.4	17.3	17.1	18.1	17.6	18.5	18.5	18.1	19.2	17.5
std	6.4	7.0	6.8	6.0	6.4	6.2	6.8	7.2	5.2	5.4
min	1.4	-1.7	-0.4	1.2	0.1	2.3	1.5	-1.4	5.7	3.0
max	43.8	44.9	44.7	42.9	44.1	43.5	46.4	46.0	40.8	39.6
Wind speed [m/s]										
mean	3.3	2.5	2.1	3.1	3.2	2.4	2.2	2.8	5.7	2.8
std	2.3	2.2	1.5	2.2	1.8	1.8	1.7	2.2	2.7	1.2
min	0.0	0.0	0.0	0.0	0.0	0.0	0.0	0.0	0.0	0.0
max	12.1	11.7	8.2	11.1	11.8	10.0	11.0	12.1	16.0	11.2

The annual CDH, namely the sum of the hourly values over the considered year, is represented in Figure 2 evidencing that the highest cooling demand is expected for Richmond (RM) and Penrith Lakes (PL), whereas Terrey Hills (TH) station has almost half the CDH value compared to the Richmond (RM) and Penrith Lakes (PL) stations.

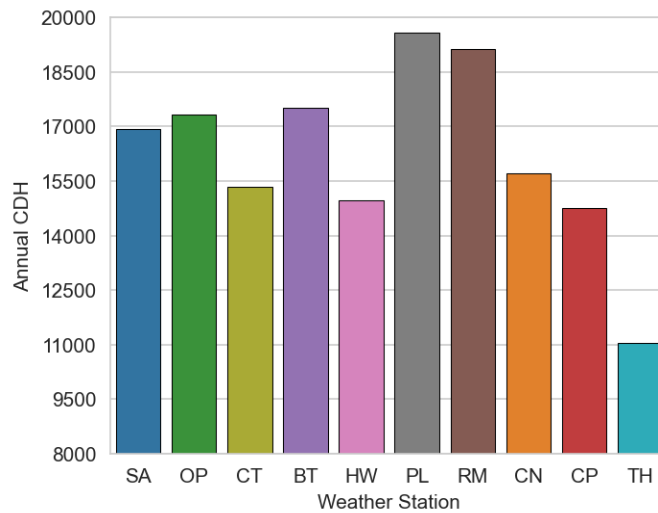


Figure 2. Annual CDH for each weather station

PV cell operating temperatures at the different weather stations and as a function of the mounting configurations

The median value for PV cell operating temperatures across all configurations ranges from about 30°C for the open-rack configurations to about 35°C for the close roof and insulated back mount. The maximum temperatures of the open rack configurations range between 65°C and 70°C, those of the close roof mount configuration are between 80°C and 90°C, whereas the insulated back configuration can reach temperatures up to 90°C and 100°C. As expected, the highest PV operating cell temperatures are found in Penrith Lakes (PL) which is characterized by the highest maximum air temperature and by low wind speed values. On the contrary, despite having the highest average mean annual air temperature

value, Sydney Airport (SA) shows the lowest operating cell temperature values thanks to the beneficial cooling effect of the sea breeze.

The normalized efficiency is calculated at an hourly timestep for each weather station and is plotted against the PV cell operating temperatures. Figure 3 illustrates the results for the Penrith Lakes (PL) weather station only for brevity, but similar results are obtained across the analysed weather stations. As it can be observed, for open rack configurations, the cell temperature values can reach up to 70°C, leading to a decrease in normalized efficiency down to 0.75. Conversely, for close roof mount and insulated back configurations, where cell temperatures can rise up to 90°C and about 100°C, respectively, the normalized efficiency may decline by up to less than 0.65.

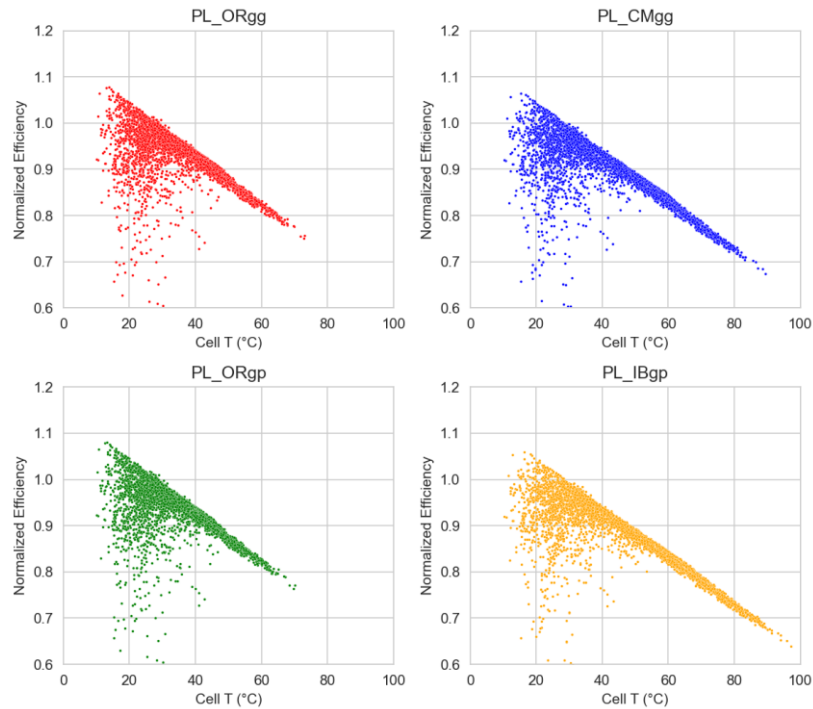


Figure 3. Normalized efficiency and PV cell operating temperature for PL weather station

PV temperature derating at the different weather stations and as a function of the mounting configurations

The temperature derating (TD) quantifies the deviation of PV power output from the standard test cell temperature conditions ($T_c=25^\circ\text{C}$). As expected, the insulated back configuration (IB) displays the highest temperature derating, with an average annual value of approximately -0.10 compared to -0.08 for the close roof mount configuration (CM). In contrast, the open-rack configurations (OR) exhibit negligible temperature deratings, generally lower than -0.05. Among the different weather stations, the impact of temperature is more pronounced in western stations (PL, RM, and CP) and in Sydney Olympic Park (OP), which are characterized by lower wind speed values. Conversely, Sydney Airport (SA) is the least impacted by temperature derating.

Observing the daily average values of TD in Penrith Lakes (PL) weather station, which are plotted in Figure 4, it can be seen that during extremely hot days occurring from November to February, the TD can reach values as low as about -0.40.

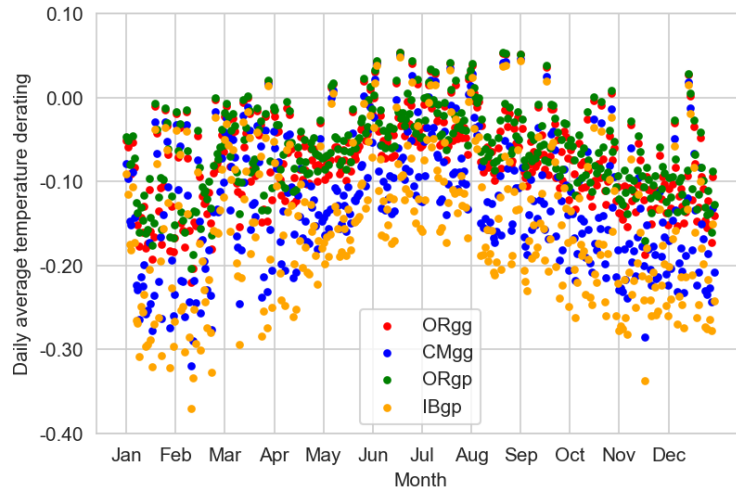


Figure 4. Daily average temperature derating in PL depending on the different mounting configurations

PV Performance Ratio and Cooling Degree Hours

To investigate the impact of high temperature conditions on PV efficiency as well as on cooling demand during the summer months (from December to February), the daily performance is calculated for each scenario to analyse its relationship with the cumulated daily values of Cooling Degree Hours (CDH). The results are shown in Figure 5 where the black line shows the linear correlation between the two variables and the related Pearson correlation coefficients (R-Pearson) are calculated for each case. All figures show an evident negative relationship between the daily performance ratio and CDH with R-Pearson values ranging from -0.67 for the insulated back configuration to -0.79 for the open rack configuration with glass/cell/polymer. A higher cooling demand corresponds to a decrease in PV performance ratio, which varies from a minimum value of about 0.80 for the open rack configuration to about 0.70 for the insulated back configuration.

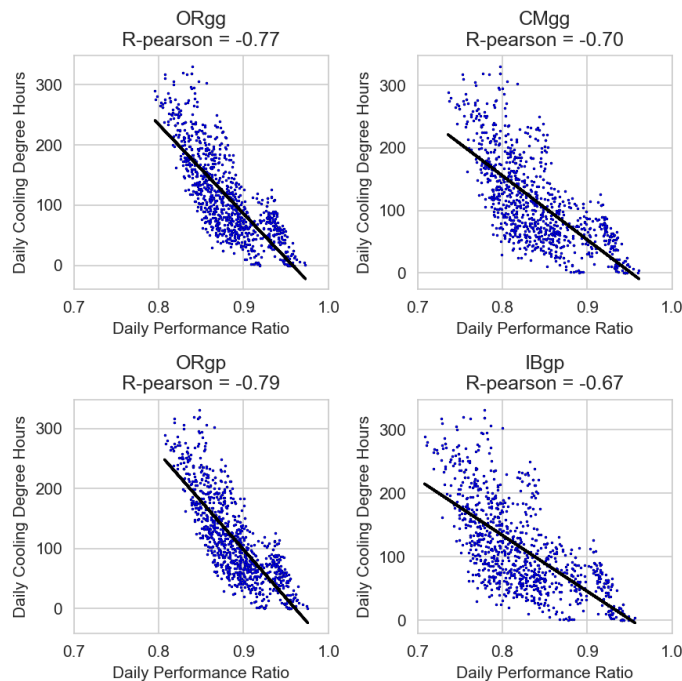


Figure 5. Daily performance ratio and cumulative daily Cooling Degree Hours as a function of the different mounting configurations

PV Efficiency and Power Production

Figure 6 shows the hourly minimum, mean, and maximum values of PV efficiency during the month of February (red) and July (blue) for the worst case, namely insulated back mounting configuration in Penrith Lakes (PL) weather station. As it can be noticed, in February PV efficiency exhibits significantly lower values compared to July with differences ranging from 0.01 to 0.02.

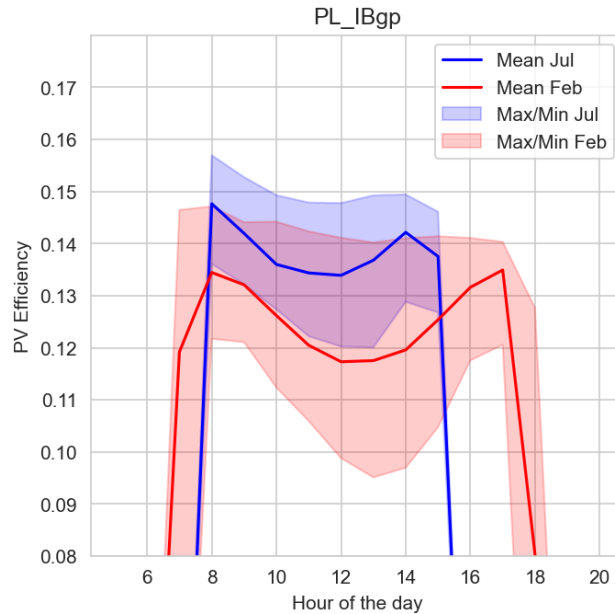


Figure 6. Hourly PV efficiency statistics (minimum, mean, and maximum values) in February (red) and in July (blue) for the insulated back mounting configuration in PL weather station.

When analyzing the annual power production, the impact of different weather conditions on the total power production is not particularly significant. The highest power production values are achieved in Sydney Airport (SA), with a total yearly power production ranging from 219 kWh/m² year for the ORgp configuration to 202 kWh/m² year for the IBgp case. The lowest production values are observed in Penrith Lakes (PL), ranging from 214 kWh/m² year (ORgp) to 194 kWh/m² year (IBgp). The results indicate that, on average, weather conditions have only a 2.7% impact on the annual power production.

Regarding the impact on power production, the mounting configuration plays a more significant role, especially during the hottest months. To assess this impact, the monthly power production (average of all weather stations) is compared as a function of the mounting configuration. The mounting configuration with the highest power production is ORgp, which benefits from lower temperatures. Conversely, the least productive configuration is IBgp, which experiences a decrease in monthly power production ranging from a minimum of 7.0% in March to a maximum of 9.5% in November.

Conclusions

This study investigated the thermal and electrical performance of four different PV module installation conditions near Sydney using the Sandia PV array performance model and meteorological data from 11 nearby weather stations. Results indicate that extremely hot weather significantly reduces module performance, with the normalized PV efficiency decreasing from 0.75 for the open rack configuration to about 0.60 for the insulated back. The open-rack configuration exhibits the highest power production, while the insulated back configuration shows an 8% decrease in power production as a yearly average. The study

highlights the importance of sea breezes in cooling the coastal areas of the city, benefiting PV systems located in these areas such as the Sydney Airport. Conversely, PV systems located in western regions of the city, such as Penrith Lakes, experience extremely high temperatures that exacerbate the negative impacts of UHIs on urban environments and PV systems. However, the local climate differences only impact PV power production by 3%, but this effect could become more pronounced in the future due to urbanization and the increase in heatwave intensity and frequency. The study also finds that the insulated back configuration exhibits the highest temperature derating, with a potential decrease of up to -50% compared to standard test cell temperature conditions. In conclusion, this study provides important insights into the performance of PV systems in urban areas and highlights the need for further research to optimize their installation and operation in the face of changing climatic conditions.

References

- Australian Energy Market Operator (AEMO). (2019). Electricity Demand Forecasting Methodology Information Paper Important notice PURPOSE, (August).
- Barron-gafford, G. A., Minor, R. L., Alle, N. A., Cronin, A. D., Brooks, A. E., & Pavaozuckerman, M. A. (2016). The Photovoltaic Heat Island Effect: Larger solar power plants increase local temperatures. *Nature Publishing Group*, (May), 1–7. Retrieved from <https://doi.org/10.1038/srep35070>
- Berardi, U., & Graham, J. (2020). Investigation of the impacts of microclimate on PV energy efficiency and outdoor thermal comfort. *Sustainable Cities and Society*, 62(July), 102402. Retrieved from <https://doi.org/10.1016/j.scs.2020.102402>
- Founda, D., & Santamouris, M. (2017). Synergies between Urban Heat Island and Heat Waves in Athens (Greece), during an extremely hot summer (2012). *Scientific Reports*, 7(1), 1–11. Retrieved from <https://doi.org/10.1038/s41598-017-11407-6>
- Hibbard, K. ., Hoffman, F. M., Huntzinger, D., & West, T. O. (2017). Ch. 10: Changes in Land Cover and Terrestrial Biogeochemistry. *Climate Science Special Report: Fourth National Climate Assessment, Volume I. Climate Science Special Report: Fourth National Climate Assessment, Volume I, 1, 277–302*. Retrieved from <https://doi.org/10.7930/J0416V6X.U.S>.
- King, D. L., Boyson, W. E., & Kratochvil, J. A. (2004). Photovoltaic array performance model. *Sandia Report No. 2004-3535, 8, 1–19*. Retrieved from <https://doi.org/10.2172/919131>
- Koschier, L., & Egan, R. (2021). *National Survey Report of PV Power Applications in Australia 2021*.
- Livada, I., Synnefa, A., Haddad, S., Paolini, R., Garshasbi, S., Ulpiani, G., ... Santamouris, M. (2019). Time series analysis of ambient air-temperature during the period 1970–2016 over Sydney, Australia. *Science of the Total Environment*, 648, 1627–1638. Retrieved from <https://doi.org/10.1016/j.scitotenv.2018.08.144>
- Matthew Adams, H. D. and T. T. (2015). Impacts of land-use change on Sydney’s future temperatures. *Office of Environment and Heritage*.
- Nadeem, F., Tariq, S., Haq, Z. U., & Khan, H. S. (2022). Investigating the synergies between the Urban Heat Island (UHI) and Heatwaves (HWs). *Preprints- Environmental Science and Pollution Research*, 1–32.
- Sailor, D. J., Anand, J., & King, R. R. (2021). Photovoltaics in the built environment: A critical review. *Energy and Buildings*, 253, 111479. Retrieved from <https://doi.org/10.1016/j.enbuild.2021.111479>
- Santamouris, M., Haddad, S., Fiorito, F., Osmond, P., Ding, L., Prasad, D., ... Wang, R. (2017). Urban heat island and overheating characteristics in Sydney, Australia. An analysis of multiyear measurements. *Sustainability (Switzerland)*, 9(5). Retrieved from

<https://doi.org/10.3390/su9050712>

- Wang, Yiping, Tian, W., Zhu, L., Ren, J., Liu, Y., Zhang, J., & Yuan, B. (2006). Interactions between building integrated photovoltaics and microclimate in urban environments. *Journal of Solar Energy Engineering, Transactions of the ASME*, 128(2), 168–172. Retrieved from <https://doi.org/10.1115/1.2188533>
- Wang, Yupeng, Berardi, U., & Akbari, H. (2016). Comparing the effects of urban heat island mitigation strategies for Toronto, Canada. *Energy and Buildings*, 114, 2–19. Retrieved from <https://doi.org/10.1016/j.enbuild.2015.06.046>

